ELSEVIER

Journal of Power Sources 110 (2002) 117–124

JOURNAL OF POWER SOURCES

www.elsevier.com/locate/jpowsour

The influence of carbon dioxide on PEM fuel cell anodes

F.A. de Bruijn*, D.C. Papageorgopoulos, E.F. Sitters, G.J.M. Janssen

ECN Clean Fossil Fuels, P.O. Box 1, 1755 ZG Petten, The Netherlands

Received 20 September 2001; received in revised form 30 March 2002; accepted 3 April 2002

Abstract

The influence of CO_2 on the performance of PEM fuel cells was investigated by means of fuel cell experiments and cyclic voltammetry. Depending on the composition and microstructure of the fuel cell anode, the effect varies from small to significant. Adsorbed hydrogen plays a dominant role in the formation of CO-like species via the reverse water–gas shift reaction. Platinum sites which are not utilized in the electrochemical oxidation of hydrogen are thought to catalyze this reverse-shift reaction. Alloying with ruthenium suppresses the reverse-shift reaction.

Keywords: PEM fuel cell (PEMFC); Reformate; CO_2-tolerance; Reverse water–gas shift

1. Introduction

The wide-spread application of PEM fuel cells for transportation and residential use implies the usage of ready available fuels as gasoline, natural gas and methanol instead of pure hydrogen [1]. Hydrogen is generated in the fuel cell system by the consecutive reforming and cleaning of carbon based fuels leading to fuel cell fuels containing hydrogen with concentration of only 30–75%, depending on the primary fuel and the reforming process used [2–5]. Other main gas components are carbon dioxide, nitrogen, water, incompletely converted fuel and carbon monoxide [5,6], while trace amounts of ammonia [1], hydrogen cyanide [1] and hydrogen sulfide [1] are reported as well.

Both sulfur containing compounds [7,8] and carbon monoxide [8–10] have already at concentration levels of 1–10 ppm a measurable negative influence on the catalyst performance, while ammonia was demonstrated to have an irreversible effect on the proton conductivity of the electrode [11].

Apart from its dilution effect, methane is regarded to be inert [12]. The influence of carbon dioxide on PEM fuel cell performance, which can be present in concentrations of up to 25%, is only described in a limited number of papers [9,13,14], primarily because its effect is thought to be negligible compared to that of CO.

While carbon dioxide itself is regarded as inert, the formation of carbon monoxide by a reverse water–gas shift reaction leads to a negative impact of carbon dioxide on the performance of fuel cell anodes [9,13,14]. As the concentration of carbon dioxide is in the order of 10–20%, already a very small reverse water–gas shift can lead to carbon monoxide concentrations which are comparable to the concentration directly emitted by the fuel cell processor, up to a concentration level of 10–100 ppm [15].

The present paper focuses on the effect of carbon dioxide on fuel cell performance at conditions relevant for stationary and mobile applications, as studied by the combination of fuel cell experiments, studies of carbon dioxide interaction with platinum and platinum–ruthenium surfaces by cyclic voltammetry and thermodynamic calculation of the carbon monoxide equilibrium concentration as a function of cell temperature and the anode gas composition.

2. Experimental

2.1. Fuel cell MEA preparation

In all fuel cell experiments reported in this paper, Nafion 105 was used as a membrane, and pre-fabricated 0.35 mg Pt/cm^2 double sided ELAT gas diffusion electrodes from E-TEK were used as cathode. The electrode geometry consisted of circular electrodes with an electrode area of 8 cm^2. For the anode, both ECN electrodes and pre-fabricated electrodes from E-TEK of various noble metal composition and noble metal loading were used, see Tables 1 and 2.

In case of self-made electrodes, a catalyst ink containing E-TEK 40 wt.% Pt or Pt-Ru supported on vulcan XC72,

* Corresponding author. Tel.: +31-224-56-4089; fax: +31-224-56-3615.
E-mail address: debruijn@ecn.nl (F.A. de Bruijn).

0378-7753/02/$ – see front matter
PII: S0378-7753(02)00227-6

Table 1
Relative fuel cell performance at 0.5 V for various fuel cell anode compositions vs. gas composition

Electrode	Anode gas composition			
	Pure H_2	90% H_2:10% CO_2	80% H_2:20% CO_2	60% H_2:40% CO_2
0.35 mg Pt/cm^2, E-TEK ELAT	1	0.74 ± 0.01	0.72 ± 0.01	0.63 ± 0.03
1.0 mg Pt/cm^2, E-TEK ELAT	1	0.81 ± 0.06	0.67 ± 0.05	0.53 ± 0.01
0.35 mg Pt-Ru/cm^2, E-TEK ELAT	1	0.92 ± 0.04	0.89 ± 0.06	0.79 ± 0.06
0.35 mg Pt/cm^2, thin-film electrode	1	0.93 ± 0.01	0.93 ± 0.02	0.88 ± 0
0.35 mg Pt-Ru/cm^2, thin-film electrode	1	0.90 ± 0.04	0.89 ± 0.04	0.85 ± 0.04
0.20 mg Pt/cm^2, thin-film electrode	1	0.94 ± 0.02	0.92 ± 0.02	0.89 ± 0.03

Cell temperature: 65 °C; anode and cathode humidified at 65 °C; 1.5 bar; hydrogen stoichiometry = 1.5; air stoichiometry = 2.0; cathode = 0.35 mg Pt/cm^2, E-TEK ELAT; membrane: Nafion 105; performance at pure hydrogen = 1.

solubilized Nafion and a suitable solvent was applied on a double sided E-TEK ELAT carbon-only gas diffusion electrode. The Nafion:catalyst ratio amounted to 1:4 on a dry basis in all self-made electrodes, further on referred to as ''thin-film electrodes''.

Prior to the assembly of the electrodes and membrane, both the pre-fabricated and the thin-film electrodes were impregnated with a 5% Nafion solution resulting in an extra Nafion loading of 1 mg/cm^2. MEAs were manufactured by hot-pressing the anode and cathode on the membrane at a pressure of 35 bar (g) at a temperature of 135 °C during 90 s.

2.2. Fuel cell experiments

Fuel cell experiments reported in this paper were performed at H_2:CO_2 ratios ranging from 100:0 to 60:40, at cell temperatures of 65 and 80 °C and at an absolute pressure of 1.5 bar. The anode and cathode gas were humidified at cell temperature by membrane humidification. Prior to exposure to H_2:CO_2 mixtures, all cells have been run on pure hydrogen for at least 18 h at 1.5 bar and 65 °C at a constant load of 0.5 V.

In all experiments a hydrogen stoichiometry of 1.5 and an oxygen stoichiometry of 2 were used. Performance data shown in all figures are obtained in the steady state, unless stated otherwise.

Table 2
Performance loss at 0.5 V for various fuel cell anode compositions vs. temperature

Electrode	Relative performance when using 80% H_2:20% CO_2 instead of 100% H_2	
	65 °C	80 °C
0.35 mg Pt/cm^2, E-TEK ELAT	0.72 ± 0.01	0.70 ± 0.02
1.0 mg Pt/cm^2, E-TEK ELAT	0.67 ± 0.05	0.61 ± 0.01
0.20 mg Pt/cm^2, thin-film electrode	0.92 ± 0.02	0.87 ± 0.01
0.35 mg Pt/cm^2, thin-film electrode	0.93 ± 0.02	0.85 ± 0.01
0.35 mg Pt-Ru/cm^2, E-TEK ELAT	0.89 ± 0.06	0.93 ± 0.05
2.0 mg Pt-Ru/cm^2, E-TEK ELAT	0.91 ± 0.03	0.95 ± 0.04
0.35 mg Pt-Ru/cm^2, thin-film electrode	0.89 ± 0.04	0.92 ± 0.02

Anode and cathode humidified at 65 °C; 1.5 bar; hydrogen stoichiometry = 1.5; air stoichiometry = 2.0; cathode = 0.35 mg Pt/cm^2, E-TEK ELAT.

2.3. Cyclic voltammetry experiments

The influence of CO_2 on Pt and Pt-Ru supported by vulcan XC72 was studied by cyclic voltammetry. Electrodes which are representative for the fuel cell anodes were obtained by applying catalyst containing inks, normally used for the fabrication of fuel cell electrodes, on a smooth platinum foil with an area of approximately 3 cm^2. Platinized platinum was used as counter electrode, Hg/Hg_2SO_4 as a reference electrode. All reported potentials are referred to the reversible hydrogen electrode (RHE). A 1 N H_2SO_4 was used as electrolyte. A computer controlled Autolab PGSTAT 20 potentiostat/galvanostat was used from Ecochemie.

After establishing the cleanliness of the solution and the catalyst containing working electrode, the latter was exposed to carbon dioxide at fixed potential during a time sufficient to reach saturation coverage. After exposure to CO_2, the coverage by adsorbates was determined in the nitrogen saturated electrolyte by the recording of a cyclic voltammogram between 0.018 and 1.26 V versus RHE at a scan rate of 5 mV/s. The influence of CO_2 exposure was investigated at adsorption potentials ranging from 0 to 0.4 V versus RHE and at temperatures between 25 and 75 °C.

3. Results

3.1. Thermodynamics

The equilibrium concentration of carbon monoxide resulting from the reaction of CO_2 and H_2 can be calculated from the equilibrium constant of the water–gas shift reaction:

$$CO(g) + H_2O(g) \Leftrightarrow CO_2(g) + H_2(g)$$

with:

$$\frac{P_{CO}}{P_{tot}} = \frac{(P_{CO_2}/P_{tot})(P_{H_2}/P_{tot})}{K(P_{H_2O}/P_{tot})}$$

In relation to PEM fuel cell conditions, the most relevant temperature range is between 40 and 80 °C, the anode gas being partially to fully saturated with water, the pressure ranging from 1 to 3 bar.

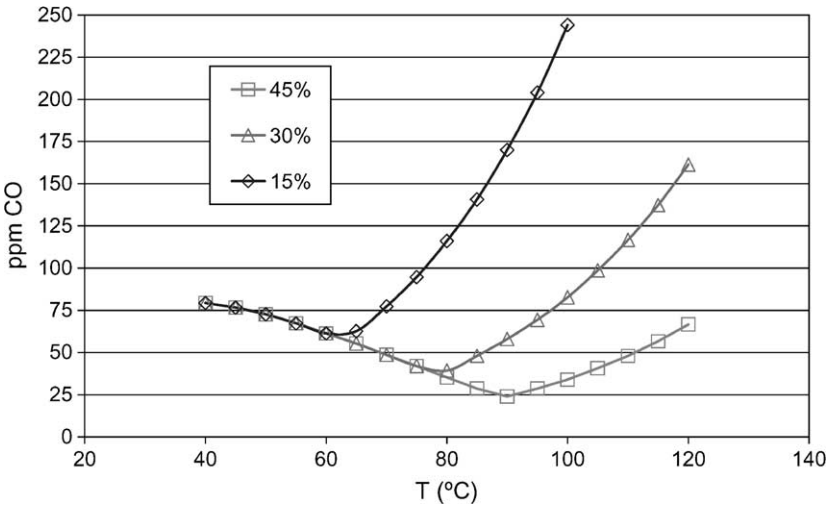

Fig. 1. Equilibrium concentration of carbon monoxide in water–gas shift reaction as a function of temperature at various water concentrations, at a H_2:CO_2 ratio of 3:1 at a pressure of 1.5 bar.

Fig. 1 gives the calculated CO concentration versus temperature at various molar water concentrations at an absolute pressure of 1.5 bar. The H_2:CO_2 ratio was fixed to 3, which is representative for a methanol based reformate. For hydrocarbon based feedstocks, the H_2:CO_2 ratio will be close to 2. The value of the equilibrium constant K was calculated on the basis of data given in [16].

Two different regions can be discerned in Fig. 1, one being at temperatures where all the water is in the vapor state, the other being at temperatures where water is both in the liquid and the vapor state.

As the reverse-shift reaction is an endothermic reaction, a rise in temperature leads to an increase in the carbon monoxide equilibrium concentration provided the water concentration is constant.

Below the temperature where the water starts to condense, a decrease in temperature leads to an increase of the equilibrium concentration of carbon monoxide as a result of decreasing water concentration in the gas phase. Below 60 °C, the water vapor pressure is lower than that corresponding to a water content in the gas phase of 30 mol%, resulting in all three lines merging together.

The most important conclusion which can be drawn from Fig. 1 is that, based on thermodynamics, the CO being produced by the reverse water–gas shift reaction taking place in the fuel cell itself, could be in the range of 20–50 ppm. Note that this is higher than the CO outlet from the fuel processor as a result of a selective oxidation unit which can lower the CO concentration to less than 10 ppm [2].

3.2. Fuel cell experiments

3.2.1. Influence of CO_2 concentration

The influence of the CO_2 content in the anode fuel is shown in Fig. 2, for standard platinum gas diffusion electrodes as obtained from E-TEK. At a CO_2 content of 20%, which is present in most reformate streams, the performance loss at 0.5 V amounts to 30%.

Table 1 gives the relative performance of the fuel cells, as calculated from steady state fuel cell current densities, for various anode compositions as a function of the anode gas composition at a fuel cell temperature of 65 °C and a pressure of 1.5 bar.

In a different fuel cell configuration, at 1.2 bar and 65 °C, using an E-TEK ELAT Pt-Ru anode with a loading of 0.35 mg/cm^2, it was established that diluting the hydrogen feed with nitrogen did not lead to any performance loss up to nitrogen concentrations of 40%, when the hydrogen stoichiometry was kept constant. Diluting the hydrogen with CO_2 to a H_2:CO_2 ratio of 80:20 in the same setup led to a performance loss of 7%. Further addition of 10 ppm CO to this H_2:CO_2 mixture led to a performance loss of 22%.

Clearly, CO_2 has, especially in the case of pre-fabricated Pt electrodes, a negative effect on the performance which is much larger than can be expected from a mere dilution effect.

3.2.2. Influence of temperature

At a constant CO_2 content of 20%, the cell temperature was varied while keeping anode and cathode gas saturated with water. The absolute performance of the cells in this study showed an increase of 30–100 mA/cm^2 when increasing the temperature from 65 to 80 °C, both with and without CO_2 in the anode feed.

Table 2 shows for all different types of anodes the performance loss when switching from pure hydrogen to 80% hydrogen:20% carbon dioxide at both 65 and 80 °C. For all anodes containing platinum as the catalyst, an increase in temperature leads to a worse tolerance towards CO_2. For the anodes containing Pt-Ru as catalyst, an increase in temperature leads to a better tolerance towards CO_2.

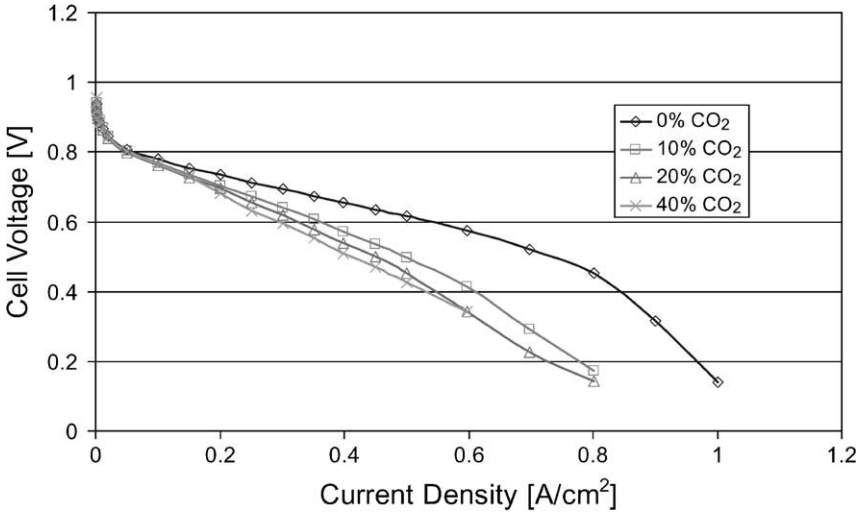

Fig. 2. Polarization curve of fuel cell at various CO_2 concentrations. Anode = cathode = 0.35 mg Pt/cm^2 E-TEK ELAT gas diffusion electrode, Nafion 105. $T_{cell} = T_{hum} = 65$ °C. $P = 1.5$ bar.

3.3. Cyclic voltammetry

3.3.1. CO_2 adsorption on Pt/vulcan electrodes

Cyclic voltammetry is an ideal technique to study adsorption phenomena at platinum electrode surfaces. The degree of coverage can directly be calculated from the inhibition of UPD hydrogen adsorption/oxidation while the potential at which the adsorbate is oxidized gives insight in whether the adsorbate can be removed under normal fuel cell conditions.

Fig. 3 gives the cyclic voltammogram of a 40 wt.% platinum on carbon catalyst which is applied from a fuel cell electrode ink on a platinum foil in an argon saturated 0.5 M H_2SO_4 solution. All features associated with the adsorption/oxidation of UPD hydrogen and the formation and subsequent reduction of a surface oxide layer on the platinum particles are clearly distinguishable. The gray area is used for the calculation of the degree of coverage by adsorbates (θ_{ads}) formed by exposure to CO_2 by using:

$$\theta_{ads} = 1 - \frac{Q^{H}_{ads}}{Q^{H}_{clean}}$$

in which Q^{H}_{ads} represents the charge associated with the oxidation of adsorbed hydrogen after adsorption of CO_2 and Q^{H}_{clean} the charge associated with the oxidation of adsorbed hydrogen in a clean sulfuric acid solution.

The potential of the electrode determines the coverage of hydrogen and oxygen on the surface. By this means, adsorption at various potentials gives insight in the influence of, in this case, the degree of coverage of hydrogen atoms on the adsorption of carbon dioxide on a platinum surface.

Fig. 4 shows the influence of the electrode potential at which the exposure to carbon dioxide takes place on the

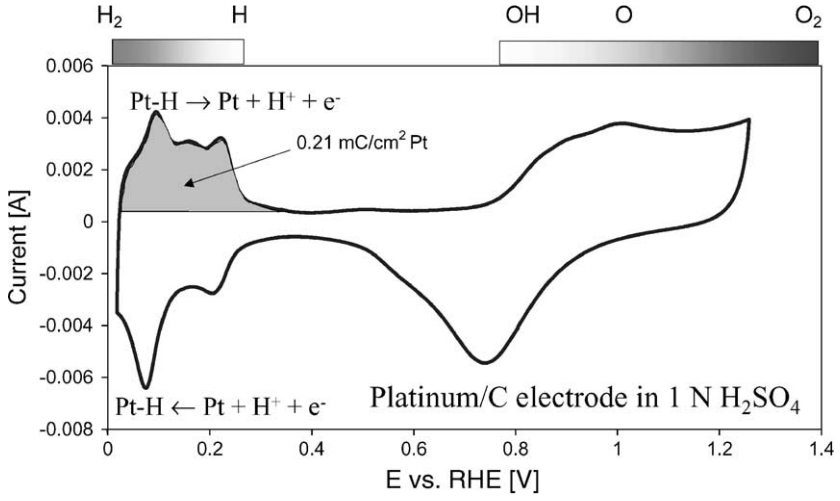

Fig. 3. Cyclic voltammogram of 40 wt.% Pt/vulcan XC72, deposited from electrode ink on platinum foil. Scan rate = 5 mV/s. Nitrogen saturated 0.5 M H_2SO_4. $T = 25$ °C.

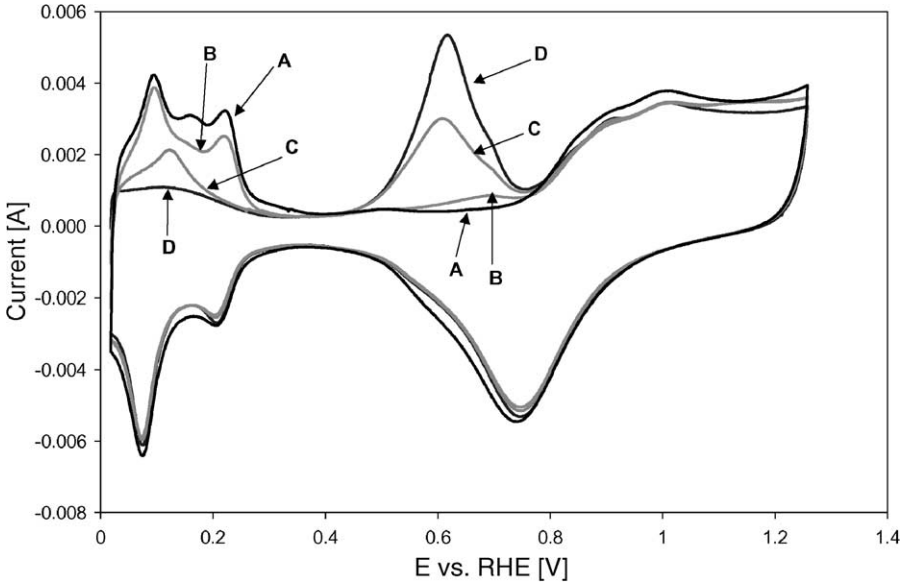

Fig. 4. Cyclic voltammogram of 40 wt.% Pt/vulcan XC72, deposited from electrode ink on platinum foil. Scan rate = 5 mV/s. Nitrogen saturated 0.5 M H_2SO_4, after exposure of electrode to CO_2 bubbling through the electrolyte, at various potentials: (A) clean, no adsorption; (B) adsorption at 0.36 V; (C) adsorption at 0.15 V; (D) adsorption at 0 V. $T = 25$ °C.

amount of adsorbed species formed. Exposure of the platinum surface to CO_2 at a potential of 0.36 V corresponds to the situation where the platinum is free from adsorbed hydrogen. Adsorption at this potential does lead to a certain reduction of platinum sites available for the adsorption of hydrogen and to a small amount of adsorbed species which can be oxidized at potentials higher than 0.6 V. Lowering of the adsorption potential leads to a drastic increase of the degree of coverage by adsorbed species and to an increase of the oxidation charge of adsorbed species. Exposure to CO_2 at 0 V leads to a degree of coverage by adsorbed species of 0.8.

As is often seen, the ''strongly adsorbing'' platinum sites are occupied preferentially. However, in this case it seems that the weakly adsorbed hydrogen, formed at potentials below 0.2 V, is especially effective in the formation of adsorbed species from CO_2, as especially the adsorption in the potential region between 0 and 0.2 V leads to the formation of adsorbed species. Surface diffusion of adsorbed species might be necessary in this mechanism.

Fig. 5 shows the influence of temperature on the formation of adsorbed species on platinum, at an adsorption potential of 0 V. With increasing temperature, the degree of coverage by adsorbates more or less remains constant. However, there

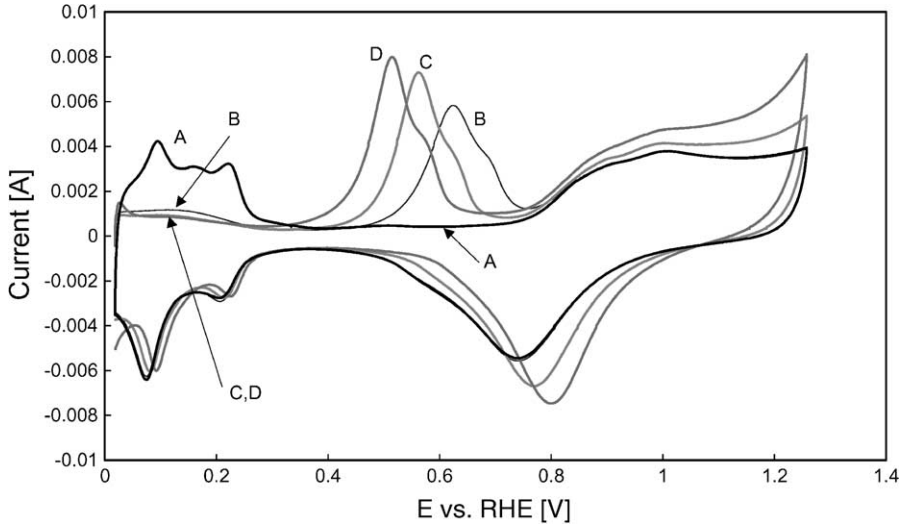

Fig. 5. Cyclic voltammogram of 40 wt.% Pt/vulcan XC72, deposited from electrode ink on platinum foil. Scan rate = 5 mV/s. Nitrogen saturated 0.5 M H_2SO_4, after exposure of electrode to CO_2 bubbling through the electrolyte, at various temperatures at 0 V: (A) clean, no adsorption; (B) adsorption at 25 °C; (C) adsorption at 50 °C; (D) adsorption at 75 °C.

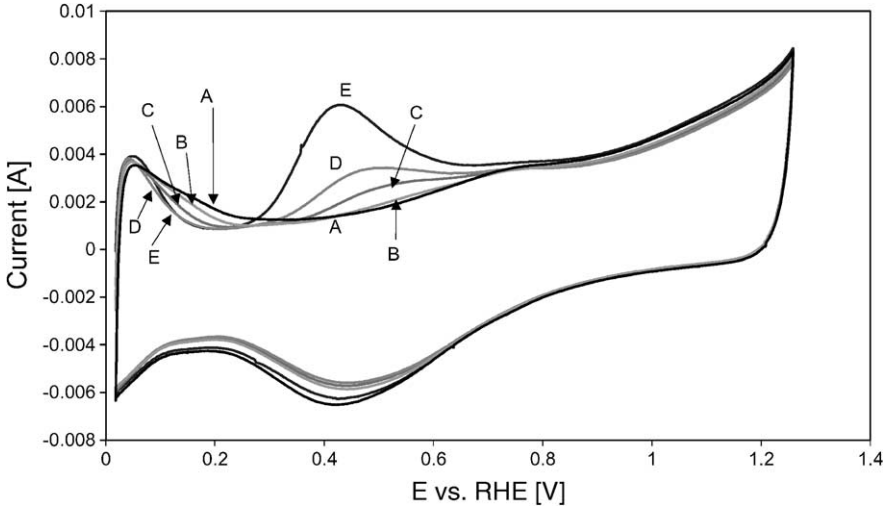

Fig. 6. Cyclic voltammogram of 40 wt.% Pt-Ru/vulcan XC72 (Pt:Ru = 1:1), deposited from electrode ink on platinum foil. Scan rate = 5 mV/s. Nitrogen saturated 0.5 M H_2SO_4, after exposure of electrode to CO_2 bubbling through the electrolyte, at various potentials: (A) clean, no adsorption; (B) adsorption at 0.2 V; (C) adsorption at 0.15 V; (D) adsorption at 0.1 V; (E) adsorption at 0 V. $T = 25$ °C.

is a large negative shift of the potential at which these adsorbates can be oxidatively removed. Besides, the oxidation charge clearly increases at increasing temperature, meaning that the oxidation charge per platinum site covered increases. This can be caused by a change in adsorption geometry of the same adsorbate as well by a change of the nature of the adsorbate.

Fig. 6 gives the cyclic voltammogram of a 40 wt.% Pt-Ru on carbon catalyst which is applied from a fuel cell electrode ink on a platinum foil in an argon saturated 0.5 M H_2SO_4 solution, both before and after exposure to CO_2 at different potentials. The determination of the degree of coverage from the hydrogen area is not as straightforward as in the case of the non-alloyed platinum surface. Therefore, only qualitative conclusions can be drawn in the case of Pt-Ru surfaces by cyclic voltammetry. It is however clear from Fig. 6 that the capacity of the surface for hydrogen adsorption remains rather high after exposure to CO_2. The same trend is observed as in the case of the supported platinum surface, i.e. the degree of coverage by adsorbed species increases with decreasing potential, as does the charge associated with the oxidation of the adsorbed species.

Fig. 7 gives the influence of temperature on the formation and subsequent oxidation of adsorbed species upon exposure

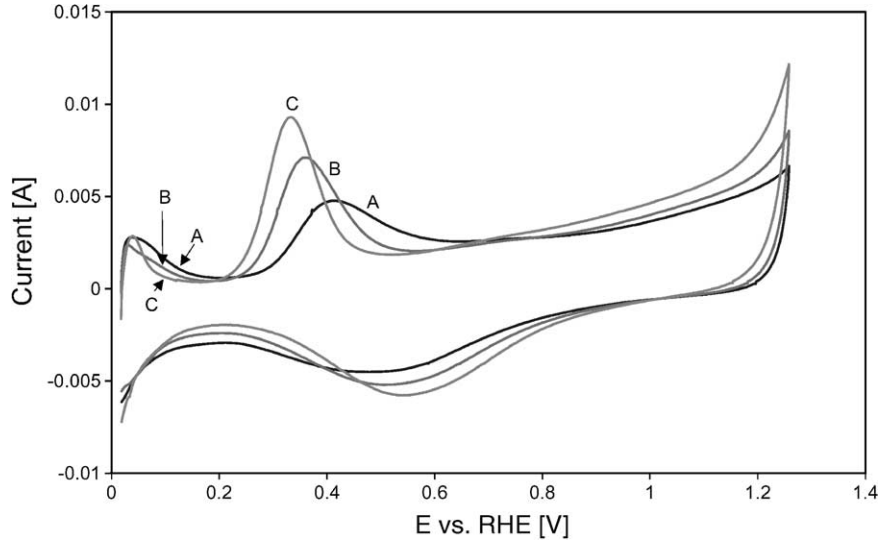

Fig. 7. Cyclic voltammogram of 40 wt.% Pt-Ru/vulcan XC72 (Pt:Ru = 1:1), deposited from electrode ink on platinum foil. Scan rate = 5 mV/s. Nitrogen saturated 0.5 M H_2SO_4, after exposure of electrode to CO_2 bubbling through the electrolyte at 0 V, at various temperatures: (A) clean, no adsorption; (B) adsorption at 25 °C; (C) adsorption at 50 °C; (D) adsorption at 75 °C.

to CO_2 at 0 V. In the case of Pt-Ru, an increase of temperature does lead to a higher degree of coverage, and to a negative shift of the potential at which the adsorbate is being oxidized.

4. Discussion

Both cyclic voltammetry and fuel cell performance data show that CO_2 in large concentrations can have a clear negative influence on fuel cell anodes. The most likely effect on the platinum or platinum ruthenium surface is the "surface-equivalent" of the water–gas shift reaction [13]:

$$2Pt + H_2 \rightarrow 2PtH$$

$$CO_2 + 2PtH \rightarrow \text{'Pt=CO'} + H_2O + Pt$$

The adsorption of CO_2 itself seems unimportant, as the exposure of a platinum surface to CO_2 in the double layer region, where adsorbed hydrogen is absent, does not lead to a significant poisoning of the platinum surface, see Fig. 4. The adsorption of neutral molecules is generally maximal in the double layer region, where the competition with adsorbed charged species and water molecules is minimal. The direct electrochemical reduction of CO_2 to CO has a standard potential of −0.2 V, meaning that its occurrence at potentials of 0 V and higher is quite unlikely.

The reverse water–gas shift involves the surface reaction of CO_2 with adsorbed hydrogen and yields CO. Cyclic voltammetry has shown that the exposure to CO_2 of platinum electrodes preadsorbed with a monolayer of adsorbed hydrogen leads to a surface almost completely covered by an adsorbate, and that the degree of coverage by this adsorbed species increases with increasing coverage of adsorbed hydrogen. Especially the presence of weakly adsorbed hydrogen promotes the formation of adsorbed species. The nature of the adsorbed species is investigated in more detail in another paper [17], but its characteristics are similar to that of CO, which based on the reverse water–gas shift is the expected product.

The decrease in fuel cell performance of fuel cells with non-alloyed platinum anodes is limited to 10–50%, when exposed to carbon dioxide:hydrogen mixtures with a CO_2 content of 40%. In the fuel cell anode, oxidation of molecular hydrogen in a carbon dioxide containing gas leads to steady state surface coverages of molecular hydrogen, atomic hydrogen and species associated with the adsorption of CO_2. As the electrochemical oxidation of molecular hydrogen is very fast, the steady state coverage of adsorbed hydrogen atoms is very low already at low over-potentials. This situation is equivalent to the exposure of CO_2 to a clean platinum surface, which is simulated in the cyclic voltammogram by adsorption at a potential in the range of 0.3–0.4 V in the case of pure platinum.

The platinum anode obtained as pre-fabricated gas diffusion electrode shows a remarkably worse tolerance towards CO_2 than the so-called thin-film electrodes which are composed from the same catalyst, being a vulcan supported platinum catalyst as supplied by E-TEK.

The initial hypothesis was that the higher platinum surface area in thin-film electrodes was the cause of the increased tolerance towards CO_2. However, the platinum loading of the electrode hardly seems to have any effect on the tolerance towards CO_2, albeit that the absolute performance of the low platinum loading electrodes is lower.

This leads to the hypothesis that the reverse shift does not take place to the same extent on the thin-film electrodes as it does on pre-fabricated E-TEK electrodes, as normally also the thin-film electrodes based on platinum-carbon catalysts are very sensitive to small amounts of carbon monoxide. In the so-called thin-film electrodes, the percentage of platinum which actually participates in the electrochemical reaction is known to be higher than in the case of standard catalyzed gas diffusion electrodes [18]. In the case of gas diffusion electrodes, solubilized Nafion is introduced on the electrode from the top of the electrode and will penetrate the electrode only partially. Uncovered platinum is likely to coexist with Nafion-covered platinum. It is supposed to be this uncovered platinum which is capable of catalyzing the reverse water–gas shift reaction, as exposure to hydrogen leads to adsorbed hydrogen atoms which can not be removed electrochemically, due to the lack of electrolyte. The CO, formed on the surface by this reverse water–gas shift is in equilibrium with CO in the gas phase. It can thus be transported via the gas phase to the platinum surface which is electrochemically active in the fuel cell anode, and act as a poison in the hydrogen oxidation reaction. The situation is illustrated in Fig. 8A. Wilson et al. [14] have reported an experiment in which a gas diffusion electrode, free of Nafion, was installed in the fuel stream before the fuel cell, leading to a sharp decrease in the performance of the down stream located fuel cell. Also in this case, the platinum of the gas diffusion electrode uncoated by Nafion was held responsible for catalyzing the reverse water–gas shift reaction [14].

In the case of thin-film electrodes, the amount of uncovered platinum is much smaller, as the electrode is fabricated from an ink in which the Nafion and platinum particles are intimately mixed. On the Nafion-covered surface, adsorbed hydrogen is immediately oxidized to protons, the dissociative adsorption of molecular hydrogen being the rate-determining step (Fig. 8B). By the low amount of adsorbed hydrogen, the reverse water–gas shift is strongly suppressed, and the influence of carbon dioxide is minor. Both the much larger influence of CO_2 on the cyclic voltammogram of platinum than on fuel cell performance and the negative influence of an increase in temperature indicate that the reverse water–gas shift is kinetically hindered. In the cyclic voltammetry experiments, time of exposure to CO_2 is long enough to establish saturation coverages, while in the fuel cell, the reverse water–gas shift competes with the electrochemical oxidation of hydrogen. In spite of the decrease of the equilibrium concentration of CO with increasing

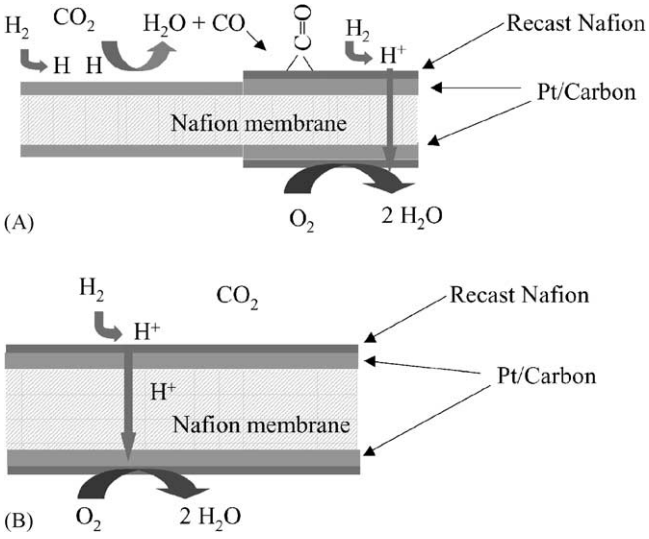

Fig. 8. Proposed mechanism for reverse water–gas shift reaction. (A) Standard E-TEK ELAT electrodes with incomplete Nafion-covered platinum surface. (B) Thin-film electrodes with completely Nafion-covered platinum surface.

temperature as calculated in Fig. 1, an increase in temperature favors the kinetics of CO formation via the reverse water–gas shift. The decrease in oxidation potential of the adsorbate is too low to be of any help, leading to a net increase of the surface coverage by CO.

Whereas, in the case of pre-fabricated E-TEK catalysts the use of platinum-ruthenium alloy catalysts for the fuel cell anode results in a much better tolerance towards CO_2, it does not in the case of thin-film electrodes. The fact that Pt-Ru based thin-film electrodes do not give a higher performance than Pt based electrodes indicates that CO is not formed in significant amounts.

From the cyclic voltammetry experiments follows that although difficult to quantify, the fraction of surface sites available for hydrogen adsorption after exposure to CO_2, both in absence and in the presence of preadsorbed hydrogen, is far much higher in the case of Pt-Ru than in the case of Pt. This is an indication for the assumption that the effect of ruthenium is mainly the suppression of the reverse-shift reaction, more than the increase of the oxidation rate of the adsorbate. An increase in temperature does lead to a little improved tolerance towards CO_2 when Pt-Ru anodes are used, apparently the decrease in oxidation potential is in this case large enough to more than compensate an increase in reverse-shift activity by an increase in temperature.

5. Conclusions

The presence of CO_2 in the anode feed of proton exchange membrane fuel cells can lead to a significant loss in performance. Especially platinum based gas diffusion electrodes, with a supposedly incomplete Nafion impregnation, are sensitive for CO_2. The negative effect is likely to be caused by the formation of CO via the reverse water–gas shift reaction on platinum sites which are not covered by Nafion. Thermodynamic calculations show that the reverse water–gas shift reaction can lead to equilibrium concentrations of CO of 20–100 ppm, both temperature and the water content of the anode feed are important parameters. The addition of ruthenium seems to suppress this reverse water–gas shift reaction. Thin-film electrodes with high electrochemical utilization are much more tolerant towards CO_2, irrespective of the noble metal composition of the anode.

Due to this effect of CO_2 on fuel cell anodes, complete removal of CO from reformate streams does not guarantee PEM fuel cell performance which is comparable to that of H_2-fed cells.

Acknowledgements

The Dutch agency NOVEM is gratefully acknowledged for subsidizing the fuel cell experiments.

References

[1] Fuel Cell Handbook, 5th Edition, US Department of Energy, 2000.
[2] A. Heinzel, B. Vogel, T. Rampe, A. Haist, P. Hübner, in: Proceedings of the Seminar on Fuel Cell, Portland OR, 2000, p. 256.
[3] A. Docter, G. Konrad, A. Lamm, in: Proceedings of the Seminar on Fuel Cell, Portland, OR, 2000, p.538.
[4] J.R. Rostrup-Nielsen, Phys. Chem. Chem. Phys. 3 (2001) 283.
[5] L.F. Brown, Los Alamos Report no. LA-13112-MS, Los Alamos, 1996.
[6] W. Wiese, B. Emonts, R. Peters, J. Power Sources 84 (1999) 187.
[7] J.B.J. Veldhuis, F.A. de Bruijn, R.K.A.M. Mallant, in: Proceedings of the Seminar on Fuel Cell, 1998.
[8] L. Pino, V. Recupero, M. Lagana, M. Minutoli, in: Proceedings of the Seminar on Fuel Cell, 1998.
[9] D.P. Wilkinson, D. Thompsett, in: Proceedings of the Second International Symposium on New Materials for Fuel Cell and Modern Battery Systems, 1997, p. 266.
[10] M. Kadowaki, S. Taniguchi, T. Matsubayashi, Y. Akiyama, K. Nishio, K. Kohno, in: Proceedings of the Seminar on Fuel Cell, 1998.
[11] F. Uribe, T. Zawodzinski, S. Gottesfeld, ECS Proc. 98 (27) (1998) 229.
[12] N. Hashimoto, H. Kudo, J. Adachi, M. Shinigawa, N. Yumaga, 32nd IECEC, no. 97116, 1997.
[13] R.J. Bellows, E.P. Marucchi-Soos, D. Terence Buckley, Ind. Eng. Chem. Res. 35 (1996) 1235.
[14] M.S. Wilson, C.R. Derouin, J.A. Valerio, S. Gottesfeld, 28th IECEC, 11203, 1993.
[15] D.P. Wilkinson, H.H. Voss, J. Dudley, G.J. Lamont, V. Basura, Patent no. WO95/08850 (1995).
[16] J.D. Cox, D.A. Wayman, V.A. Medvedev, CODATA Key Values for Thermodynamics. Seminumerical Algorithms, Hemisphere, New York, 1989.
[17] D.C. Papageorgopoulos, F.A. de Bruijn, J. Electrochem. Soc. 149 (2002) A140.
[18] M.S. Wilson, S. Gottesfeld, J. Appl. Electrochem. 22 (1992) 1.